Canadian Journal of Cardiology 35 (2019) 1523–1533

Clinical Research

Diagnostic Performance of Machine Learning Based CT-FFR in Detecting Ischemia in Myocardial Bridging and Concomitant Proximal Atherosclerotic Disease

Fan Zhou, MSc,[a,‡] Yi Ning Wang, MD,[b,‡] U. Joseph Schoepf, MD,[a,c] Christian Tesche, MD,[c,d] Chun Xiang Tang, PhD,[a] Chang Sheng Zhou, MSc,[a] Lei Xu, MD, PhD,[e] Yang Hou, MD, PhD,[f] Min Wen Zheng, MD, PhD,[g] Jing Yan, PhD,[h] Meng Jie Lu, MSc,[a] Guang Ming Lu, MD,[a] Dai Min Zhang, MD, PhD,[i] Bo Zhang, MD,[j] Jia Yin Zhang, PhD,[k] and Long Jiang Zhang, MD, PhD[a]

[a] *Department of Medical Imaging, Jinling Hospital, Medical School of Nanjing University, Nanjing, Jiangsu, China;* [b] *Department of Radiology, Peking Union Medical College Hospital, Chinese Academy of Medical Sciences and Peking Union Medical College, Beijing, China;* [c] *Division of Cardiovascular Imaging, Department of Radiology and Radiological Science, Medical University of South Carolina, Charleston, South Carolina, USA;* [d] *Department of Cardiology and Intensive Care Medicine, Heart Center Munich-Bogenhausen, Munich, Germany;* [e] *Department of Radiology, Beijing Anzhen Hospital, Capital Medical University, Beijing, China;* [f] *Department of Radiology, Shengjing Hospital of China Medical University, Shenyang, China;* [g] *Department of Radiology, Xijing Hospital, Air Force Military Medical University, Xi'an, China;* [h] *Siemens Healthcare Ltd., Shanghai, China;* [i] *Department of Cardiology, Nanjing First Hospital, Nanjing Medical University, Nanjing, Jiangsu, China;* [j] *Department of Radiology, Taizhou People's Hospital, Taizhou, Jiangsu, China;* [k] *Institute of Diagnostic and Interventional Radiology, Shanghai Jiao Tong University Affiliated Sixth People's Hospital, Shanghai, China*

ABSTRACT

Background: The diagnostic performance of coronary computed tomography angiography-derived fractional flow reserve (CT-FFR) in detecting ischemia in myocardial bridging (MB) has not been investigated to date.

Methods: This retrospective multicentre study included 104 patients with left anterior descending MBs. MB was classified as either superficial or deep, short, or long, whereas all MB vessels were further divided into <50%, 50% to 69%, and ≥70% groups, according to proximal lumen stenosis on invasive coronary angiography. Diagnostic performance and receiver operating characteristics (ROC) of CT-FFR to detect lesion-specific ischemia was assessed on a per-vessel level, using invasive FFR as reference standard. Intraclass correlation coefficient (ICC) and Bland-Altman plots were used for agreement measurement.

RÉSUMÉ

Contexte : L'efficacité diagnostique de la mesure de la reserve de flux coronaire (FFR, pour *fractional flow reserve*) par coronarographie par tomodensitométrie à déceler une ischémie causée par un pont myocardique n'a pas encore été étudiée.

Méthodologie : Cette étude multicentrique rétrospective regroupait 104 patients présentant un pont myocardique au niveau de l'artère interventriculaire antérieure. Les ponts myocardiques étaient classés comme superficiels ou profonds, courts ou longs, tandis que tous les vaisseaux présentant un pont myocardique étaient quant à eux classés dans les groupes < 50 %, 50 % à 69 %, et ≥ 70 % en fonction de la sténose proximale observée à la coronarographie invasive. L'efficacité diagnostique et la courbe ROC (pour *receiver operating characteristics*) de la mesure de la réserve de flux coronaire à détecter une ischémie propre à une lésion ont été évaluées en fonction des vaisseaux

Invasive fractional flow reserve (FFR) is considered to be the gold standard for evaluating functionally significant coronary stenosis and indicating coronary revascularization in stable coronary artery disease (CAD).[1,2] However, the implementation of invasive FFR is still underused owing to the invasive nature and the need to administer drugs that induce hyperemia and additional costs.[3] Recently, coronary CT angiography (cCTA)-derived FFR (CT-FFR) has been introduced and demonstrated high diagnostic performance in patients with stable CAD when compared with invasive FFR.[4-7] Moreover, the integration of cCTA with CT-FFR is associated with safety reduction of invasive coronary angiography (ICA)

Received for publication June 29, 2019. Accepted August 21, 2019.

‡These authors contributed equally to this study.

Corresponding authors: Dr Long Jiang Zhang, Department of Medical Imaging, Jinling Hospital, Medical School of Nanjing University, Nanjing, Jiangsu 210002, China.

E-mail: kevinzhlj@163.com

Dr Jia Yin Zhang, Institute of Diagnostic and Interventional Radiology, Shanghai Jiao Tong University Affiliated Sixth People's Hospital, #600, Yishan Rd, 200233 Shanghai, China.

E-mail: andrewssmu@msn.com

See page 1532 for disclosure information.

https://doi.org/10.1016/j.cjca.2019.08.026

Results: Forty-eight MB vessels (46.2%) showed ischemia by invasive FFR (≤0.80). Sensitivity, specificity, and accuracy of CT-FFR to detect functional ischemia were 0.96 (0.85 to 0.99), 0.84 (0.71 to 0.92), and 0.89 (0.81 to 0.94), respectively, in all MB vessels. There were no differences in diagnostic performance between superficial and deep MB or between short and long MB (all $P > 0.05$). The accuracy of CT-FFR was 0.96 (0.85 to 0.99) in ≥70% stenosis, 0.82 (0.67 to 0.91) in 50% to 69% stenosis, and 0.89 (0.51 to 0.99) in <50% stenosis ($P = 0.081$). Bland-Altman analysis showed a slight mean difference between CT-FFR and invasive FFR of 0.014 (95% limit of agreement, −0.117 to 0.145). The ICC was 0.775 (95% confidence interval, 0.685-0.842, $P < 0.001$).

Conclusions: CT-FFR demonstrated high diagnostic performance for identifying functional ischemia in vessels with MB and concomitant proximal atherosclerotic disease when compared with invasive FFR. However, the clinical use of CT-FFR in patients with MB needs further study for stronger and more robust results.

Résultats : La mesure invasive de la réserve de flux coronaire a révélé une ischémie dans 48 vaisseaux présentant un pont myocardique (46,2 %) (≤ 0,80). La sensibilité, la spécificité et la précision de la mesure de la réserve de flux coronaire par coronarographie par tomodensitométrie à détecter une ischémie fonctionnelle étaient de 0,96 (0,85 à 0,99), 0,84 (0,71 à 0,92) et 0,89 (0,81 à 0,94), respectivement, pour tous les vaisseaux présentant un pont myocardique. Aucune différence n'a été observée quant à l'efficacité diagnostique entre les ponts myocardiques superficiels et profonds, ou entre les ponts myocardiques courts et longs (valeur $p > 0,05$ dans tous les cas). La précision de la mesure de la réserve de flux coronaire par coronarographie par tomodensitométrie était de 0,96 (0,85 à 0,99) dans le cas d'une sténose ≥ 70 %, de 0,82 (0,67 à 0,91) dans celui d'une sténose de 50 % à 69 %, et de 0,89 (0,51 à 0,99) dans celui d'une sténose < 50 % ($p = 0,081$). L'analyse de Bland-Altman a révélé une différence moyenne légère de 0,014 entre la mesure de la réserve de flux coronaire par coronarographie par tomodensitométrie et la mesure invasive de la réserve de flux coronaire (limites de concordance à 95 %, −0,117 à 0,145). Le coefficient de corrélation intra-classe était de 0,775 (intervalle de confiance à 95 %, 0,685-0,842; $p < 0,001$).

Conclusions : La mesure de la réserve de flux coronaire par coronarographie par tomodensitométrie a été associée à une efficacité diagnostique élevée pour ce qui est du repérage d'une ischémie fonctionnelle au niveau des vaisseaux présentant un pont myocardique et de l'athérosclérose proximale concomitante, comparativement à la mesure invasive de la réserve de flux coronaire. L'utilisation en pratique clinique de la mesure de la réserve de flux coronaire par coronarographie par tomodensitométrie chez les patients présentant un pont myocardique doit toutefois faire l'objet d'études plus approfondies afin d'obtenir des résultats plus probants.

and costs compared with standard practice.[8] However, CT-FFR algorithms based on computational fluid dynamics (CFD) is time consuming because of the need for off-site supercomputers, which markedly limit its clinical utility.[9] Thus, the machine learning (ML)-based CT-FFR approach, using artificial intelligence algorithms to assess the functionally significant coronary lesions, has been introduced,[10-12] resulting in a significantly shorter processing time.[12] Although this ML-based CT-FFR showed similar diagnostic performance for the identification of lesion-specific ischemia compared with CFD-based CT-FFR,[13,14] the clinical implementation still remain problematic.

Myocardial bridging (MB), a congenital variant of coronary artery, is commonly seen in the left anterior descending (LAD) coronary artery.[15,16] Although MB is generally thought to be a normal variant, the vessel compression due to MB and the plaques prone to form proximal to the MB entrance may be associated with myocardial infarction.[15,16] The implementation of CFD modelling in MB is still challenging, owing to the dynamic nature of the tunneled artery with cardiac cycle. Previous studies have shown that low shear stress and flow recirculation zones may be important factors accelerating formation of atherosclerotic plaque.[17,18] Intracoronary hemodynamic assessment using FFR, especially dobutamine stress-dependent diastolic FFR quantification, has been shown to contribute to the physiological assessment of MBs.[19,20] Although CT-FFR has been used to non-invasively assess the lesion-specific ischemia, the role of CT-FFR to evaluate functional ischemia in patients with MB has never been investigated.[15]

Thus, we attempted to study the diagnostic performance of ML-based CT-FFR to detect functional ischemia in MB with invasive FFR as the reference standard.

Material and Methods

Study protocol

This retrospective study was approved by the local institutional review board, and written informed patient consent was obtained. A total of 284 patients who underwent cCTA for the evaluation of suspected or known CAD between May 1, 2015, and June 30, 2018, were prospectively enrolled from 8 centres in China. All patients were subsequently referred to ICA within 60 days of cCTA. Invasive FFR during index ICA was measured for at least 1 coronary lesion. Clinical data was recorded at the time of cCTA acquisition. MB was defined as an epicardial portion of a major coronary artery coursing

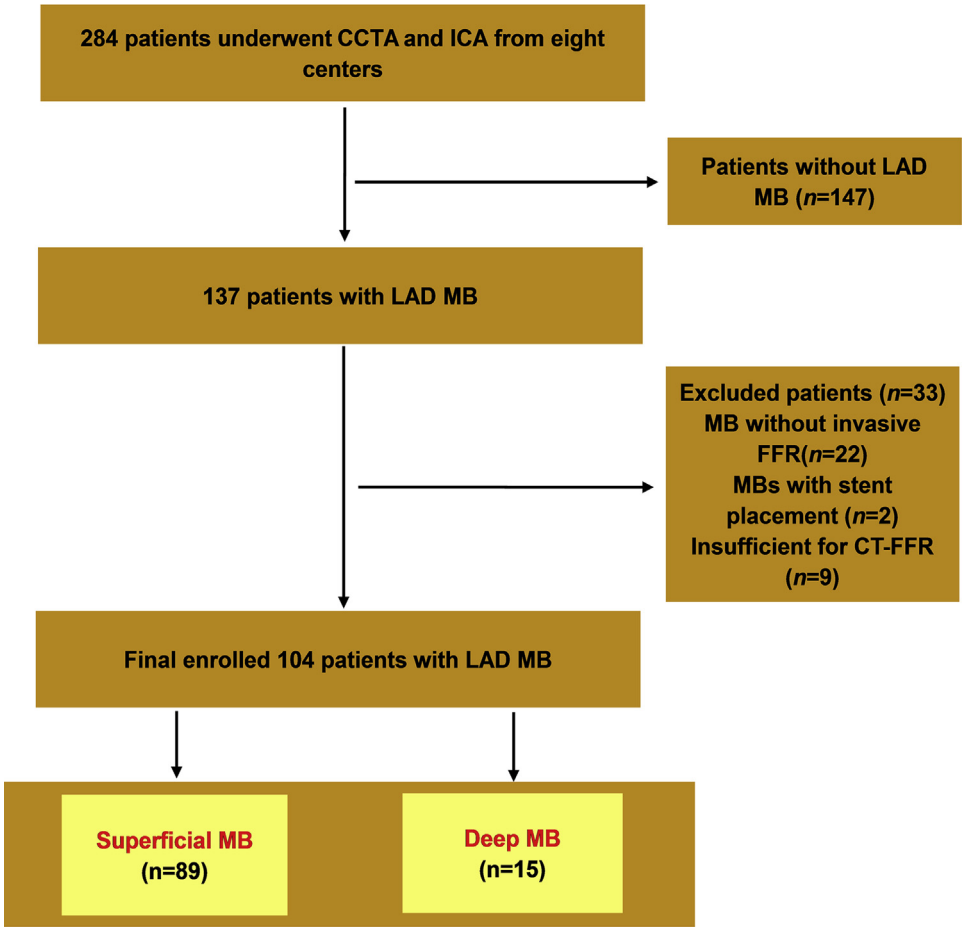

Figure 1. Flow chart of the study. CCTA, coronary CT angiography; CT-FFR, coronary computed tomography angiography derived fractional flow reserve; FFR, fractional flow reserve; ICA, invasive coronary angiography; LAD, left anterior descending coronary artery; MB, myocardial bridging.

through the myocardium on cCTA.[21] The flowchart of the population selection is presented in Figure 1.

cCTA scanning protocol

cCTA acquisition was performed using CT scanners with ≥ 64 detector rows (Somatom Definition/Flash/Force, Siemens Healthineers, Forchheim, Germany; or Aquilion One, Toshiba, Otawara, Japan) in each medical centre. All subjects received sublingual nitroglycerin (0.1 mg per dose, Nitroglycerin Inhaler; Jingwei Pharmacy Co, Ltd, Jinan, China) 3 to 5 minutes before cCTA acquisition. β-Blockers (25 mg to 75mg) were administered orally 1 hour before the examination if necessary to regulate the heart rate. The specific scanning protocols were consistent with the routine clinical practice of cCTA for each medical centre. Sixty to 65 mL of iodinated contrast agent (Ultravist 370 mg I/mL, Bayer, Schering Pharma, Berlin, Germany) was administrated by intravenous injection (4 to 5 mL/s), followed by rinsing with 20 mL to 40 mL of saline. A bolus tracking method was used to determine optimal delay time with a region of interest (ROI) placed in the aortic root. cCTA images were reconstructed with a section thickness of 0.625 mm to 0.75 mm and an interval of 0.33 mm to 0.625 mm at the optimal diastolic phase.

MB features measurements

Image analysis was performed on a dedicated workstation (Syngo.via, Siemens Healthineers, Munich, Germany) in the same medical centre. The location, depth, length, and stenosis of MB was measured at the diastolic cCTA as previous described.[22-24] According to MB depth, MBs were classified into superficial (≤ 2 mm) and deep (> 2 mm).[22] According to MB length, MBs were classified into short (≤ 3.0 cm) and long (> 3.0 cm).

CT-FFR modelling and measurements

All CT-FFR measurements were conducted on routine cCTA datasets, using cFFR version 3.2.0 (cFFR, Siemens). The cFFR software is based on a deep ML platform that has been previously trained to learn the relationship between the CT-FFR values and quantitative anatomic characteristics using a synthetically generated database of more than 12,000 3-dimensional coronary models with various degrees of coronary artery stenosis and the known outcome.[12-14] A previous study has described the calculation principle of this ML-based CT-FFR in detail.[22] CT-FFR values were determined for coronary arteries ≥ 2 mm in diameter by one observer (F.Z.), based on the location of invasive FFR measurements. Automatically generated centreline and luminal contours of the coronary

artery were verified by a more experienced observer (L.J.Z.). Both observers were blinded to the results of ICA and invasive FFR except for the measured sites.

Evaluation of the Degree of Coronary Atherosclerotic Plaque Calcification

We evaluated the degree of plaque calcification on an arterial cross-section of the most severe lesion as defined by cCTA using the number of involved calcium quadrants. Only the arterial cross-section with highest grade of plaque calcium patterns within this area was assessed to define the degree of target lesion calcification. A blinded reader (F.Z.) assessed the atherosclerotic plaque calcium as follows: (1) no calcification (no calcification present in any quadrants); (2) mild (1-quadrant calcification); (3) moderate (2-quadrant calcification); (4) severe (3-quadrant calcification); or (5) very severe (4-quadrant calcification) according to previous studies.[25,26] We further divided the patients with LAD MB and atherosclerotic plaque proximal to MB into 3 groups according to the degree of coronary calcification: no calcification, low calcification (mild/moderate calcification), and high calcification (severe/very severe calcification).

ICA and FFR measurements

Invasive coronary angiography and FFR were performed by experienced interventional cardiologists in each medical centre, according to standard practice,[27] who were blinded to CT-FFR results. FFR measurements were performed using 6F or 7F guiding catheters at 20 mm to 40 mm distal to the stenosis in vessel segments $\geq$ 2 mm. Intracoronary adenosine was injected manually through a dedicated infusion pump of either 80 μg (LAD) or 40 μg (right coronary artery) to induce hyperemia. The diameter stenosis caused by proximal atherosclerotic plaque of MB was visually recorded during ICA. According to the diameter stenosis recorded on ICA, the 104 patients were divided into 3 groups: $<$ 50% stenosis, 50% to 69% stenosis, and $\geq$ 70% stenosis. FFR $\leq$ 0.80 was considered to define functional ischemia.[9,19,28]

Statistical analysis

Statistical analysis was performed using SPSS version 19.0 (SPSS, Chicago, IL) and MedCalc version 18.2.1 (MedCalc Software, Ostend, Belgium). The normality of quantitative data was assessed using the Kolmogorov-Smirnov test. The mean $\pm$ standard deviation (SD) was used to express normally distributed quantitative variables, while the median and interquartile range (M [QU-QL]) was used to describe non-normally distributed data. Categorical variables were presented as numbers and percentages. The association between CT-FFR and FFR was assessed by Bland-Altman plots with 95% limits of agreement and intraclass correlation coefficient (ICC) ($<$ 0.2, poor; 0.2 to 0.4, fair; 0.4 to 0.6-moderate; 0.6 to 0.8, good; 0.8 to 1.0, very good).[29] One-way analysis of variance (ANOVA) was used to evaluate intergroup differences. The receiver-operating characteristic (ROC) curve with a corresponding area under the ROC curve (AUC) was performed to assess the per-vessel discrimination of functional ischemia by CT-FFR in each group, using invasive FFR as the reference standard. Comparisons of AUCs among different groups were conducted in the light of the method described by Delong et al.[30] Diagnostic sensitivity, specificity, accuracy, negative predictive value (NPV), and positive predictive value (PPV) were provided. A P value $<$ 0.05 was defined as statistically significant

Results

Patient characteristics

Patient demographics and MB features are shown in Table 1. The final patient population consisted of 104 patients with 104 LAD MB (mean age: 61.2 $\pm$ 9.1 years old, 72.1% male). Eighty-nine MBs (85.6% [89 of 104]) were superficial, and 56 MBs (53.8% [56 of 104]) were short. Proximal atherosclerotic plaques of MB were found in 103 MB vessels with luminal stenosis ranging from 30% to 90% at ICA. Ninety-seven patients had only 1 proximal atherosclerotic plaque of LAD

Table 1. Patient demographics

Basic characteristics	
Age, years	61.2 $\pm$ 9.1
Sex (male), n (%)	75 (72.1%)
Cardiovascular risk factors	
Diabetes, n (%)	26 (25.0%)
Hypertension, n (%)	58 (55.8%)
Current smoker, n (%)	40 (38.5%)
Hypercholesterolemia, n (%)	37 (35.6%)
History of CAD, n (%)	0
Previous myocardial infarction, n (%)	3 (2.9%)
Chest pain	
Typical angina, n (%)	42 (40.4%)
Atypical angina, n (%)	24 (23.1%)
Nonanginal chest pain, n (%)	5 (4.8%)
Others (dyspnea, n [%])	7 (6.7%)
Asymptomatic, n (%)	23 (22.1%)
MB features	
MB location, mm	37.4 $\pm$ 12.7
MB length, mm	28.1 (20.4-39.4)
MB depth, mm	1.0 (1.0-1.3)
MB muscle index	32.2 (22.3-48.7)
MB stenosis, %	32.1 $\pm$ 19.8
MB categories	
Superficial MB, n (%)	89 (85.6%)
Deep MB, n (%)	15 (14.4%)
Short MB, n (%)	56 (53.8%)
Long MB, n (%)	48 (46.2%)
Concomitant LAD plaque (per patient)	
No LAD plaque	1 (1%)
Proximal LAD plaque	103 (99.0%)
Plaque calcification	
No calcification, n (%)	19 (18.4%)
Mild calcification, n (%)	33 (32.0%)
Moderate calcification, n (%)	27 (26.2%)
Severe calcification, n (%)	5 (4.9%)
Very severe calcification, n (%)	19 (18.4%)
ICA stenosis	
$<$ 50% stenosis, n (%)	9 (8.6%)
50%-69% stenosis, n (%)	45 (43.3%)
$\geq$ 70% stenosis, n (%)	50 (48.1%)
FFR/CT-FFR	
FFR $\leq$ 0.80, n (%)	48 (46.2%)
CT-FFR $\leq$ 0.80, n (%)	55 (52.9%)

CAD, coronary artery disease; CT-FFR, coronary computed tomography angiography derived FFR; FFR, fractional flow reserve; ICA, invasive coronary angiography; LAD, left anterior descending coronary artery; MB, myocardial bridging.

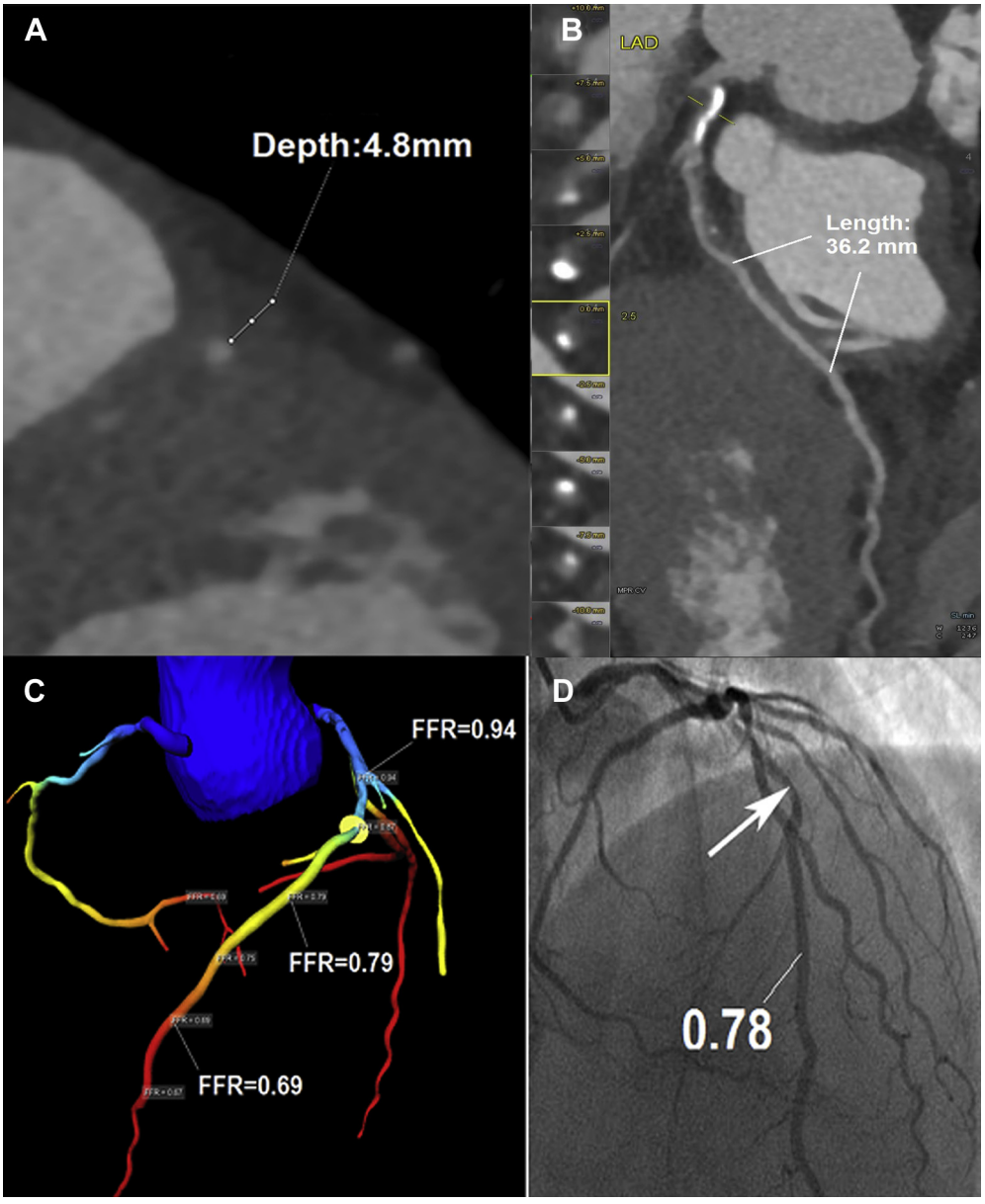

Figure 2. Coronary computed tomography angiography derived fractional flow reserve (CT-FFR) features of the left anterior descending coronary artery (LAD) with myocardial bridging (MB). Deep MB in the mid-segment of the LAD with associated moderate stenosis (70%) proximal to the MB in a 60-year-old man. (**A, B**) The MB depth is 4.8mm and the MB length is 36.2 mm. (**C**) Computational CT-FFR analysis indicates the hemodynamic significance of the LAD lesion with a CT-FFR of 0.79 in the midsegment of the MB. (**D**) Invasive coronary angiography demonstrates maximal stenosis of 70% in the proximal segment of the LAD (**arrow**). An invasive FFR value of 0.78 in the LAD confirmed the lesion-specific ischemia.

MB, whereas 6 had 2 proximal atherosclerotic plaques of MB. One patient with LAD MB had no proximal atherosclerotic plaque. We further analyzed the most severe lesion as defined by cCTA. There was no additional stenosis in the target vessel course beyond the MB. Fifty vessels (48.1% [50 of 104]) showed $\geq$ 70% diameter stenosis on ICA. Eight vessels (7.7% [8 of 104]) showed 30% to 49% diameter stenosis on ICA. Nineteen (18.4% [19 of 103]) proximal atherosclerotic plaques of MB showed no calcification. Twenty-four (23.3% [24 of 103]) proximal atherosclerotic plaques of MB showed severe or very severe calcification. CT-FFR, and invasive FFR showed functional ischemia in 55 vessel (52.9% [55 of 104] and 48 vessels (46.2% [48 of 104]), respectively. A representative case of CT-FFR assessment in 1 patient with LAD MB is shown in Figure 2.

CT-FFR diagnostic performance

The diagnostic performance of CT-FFR using invasive FFR as the reference standard is reported in Table 2. The sensitivities, specificities, accuracies, PPVs, and NPVs of CT-FFR were 0.96 (0.85 to 0.99), 0.84 (0.71 to 0.92), 0.89 (0.81 to 0.94), 0.84 (0.71 to 0.92), and 0.96 (0.85 to 0.99), respectively, in all MB vessels. No differences were shown

Table 2. Diagnostic performance of CT-FFR (≤0.80) in determining myocardial ischemia

Analysis basis	TP	TN	FP	FN	Statistical results (95% CI) Sen.	Spec.	Acc.	PPV	NPV	AUC
All MB vessels	46	47	9	2	0.96 (0.85-0.99)	0.84 (0.71-0.92)	0.89 (0.81-0.94)	0.84 (0.71-0.92)	0.96 (0.85-0.99)	0.95 (0.88-0.98)
Superficial MB	40	39	8	2	0.95 (0.83-0.99)	0.83 (0.69-0.92)	0.89 (0.80-0.94)	0.83 (0.69-0.92)	0.95 (0.82-0.99)	0.94 (0.87-0.98)
Deep MB	6	8	1	0	1.00 (0.52-1.00)	0.89 (0.51-0.99)	0.93 (0.66-1.00)	0.86 (0.42-0.99)	1.00 (0.60-1.00)	0.99 (0.77-1.00)
P value (deep vs superficial)	-	-	-	-	> 0.999	> 0.999	0.937	> 0.999	> 0.999	0.070
Short MB	23	28	3	2	0.92 (0.72-0.99)	0.90 (0.73-0.97)	0.91 (0.80-0.97)	0.88 (0.69-0.97)	0.93 (0.76-0.99)	0.98 (0.91-1.00)
Long MB	23	19	6	0	1.00 (0.82-1.00)	0.76 (0.54-0.90)	0.88 (0.74-0.95)	0.79 (0.60-0.91)	1.00 (0.79-1.00)	0.89 (0.77-0.96)
P value (short vs deep)	-	-	-	-	0.490	0.278	0.555	0.582	0.515	0.066
< 50% ICA	1	7	1	0	1.00 (0.05-1.00	0.88 (0.47-0.99)	0.89 (0.51-0.99)	0.50 (0.03-0.97)	1.00 (0.56-1.00)	-
50%-69% ICA	10	27	7	1	0.91 (0.57-1.00)	0.79 (0.62-0.91)	0.82 (0.67-0.91)	0.59 (0.33-0.81)	0.96 (0.80-1.00)	0.88 (0.75-0.96)
≥ 70% ICA	35	13	1	1	0.97 (0.84-1.00)	0.93 (0.64-1.00)	0.96 (0.85-0.99)	0.97 (0.84-1.00)	0.93 (0.64-1.00)	0.99 (0.91-1.00)
P value (< 50% vs 50%-69% vs < 70%)	-	-	-	-	0.675	0.457	0.081	<0.001	0.644	0.029

-, unavailable data; Acc., accuracy; AUC, area under the curve; CI, confidence interval; CT-FFR, coronary computed tomography angiography derived fractional flow reserve; FN, false negative; FP, false positive; ICA, invasive coronary angiography; MB, myocardial bridging; NPV, negative predictive value; PPV, positive predictive value; Sen., sensitivity; Spec., specificity; TN, true negative; TP, true positive.

between superficial and deep MB or between short and long MB for the sensitivity, specificity, accuracy, PPV, and NPV of CT-FFR ≤ 0.80 to detect hemodynamically significant stenosis (all $P > 0.05$). Among different stenosis groups, the sensitivity, specificity, accuracy, and NPV of CT-FFR ≤ 0.80 to detect hemodynamically significant stenosis showed no significant difference (all $P > 0.05$). However, the PPV (0.97 [0.84 to 1.00] vs 0.59 [0.33 to 0.81], $P = 0.001$) in the ≥ 70% stenosis group was significantly higher than that in the 50% to 69% stenosis group. The PPV showed no significant difference between the ≥ 70% stenosis group and the < 50% stenosis group (0.97 [0.84 to 1.00] vs 0.50 [0.03 to 0.97], $P = 0.104$), or between the 50% to 69% stenosis group and the <50% stenosis (0.59 [0.33 to 0.81] vs 0.50 [0.03 to 0.97], $P > 0.999$). We analyzed the discrimination of CT-FFR for functional ischemia using ROC analysis except for the < 50% stenosis group because of the relatively small sample size (n = 9). The AUCs were 0.95 (95% confidence interval [CI], 0.88-0.98, $P < 0.001$) in all MB vessels, 0.94 (95% CI, 0.87-0.98, $P < 0.001$) in superficial MB, 0.99 (95% CI, 0.77-1.000, $P < 0.001$) in deep MB, 0.98 (95% CI, 0.91-1.00, $P < 0.001$) in short MB, 0.89 (95% CI, 0.77-0.96, $P < 0.001$) in long MB, 0.88 (95% CI, 0.75-0.96, $P < 0.001$) in the 50% to 69% stenosis group, and 0.99 (95% CI, 0.91-1.00, $P < 0.001$) in the ≥ 70% stenosis group, respectively (Table 2 and Fig. 3). In our mismatch cases, 81.8% (9 of 11) of CT-FFR values ranged from 0.75 to 0.85. The detailed information about 9 false positive MB vessels and 2 false negative MB vessels is presented in Supplemental Table S1. The diagnostic performance of CT-FFR for detecting ischemia (FFR ≤ 0.80) in different calcification groups is shown in Supplemental Table S2. There were no differences for CT-FFR diagnostic performance between different calcification groups (all $P > 0.05$).

Correlation of CT-FFR with invasive FFR

Comparisons of CT-FFR with invasive FFR are showed in Figures 4 and 5. There was good correlation between CT-FFR and invasive FFR with ICC of 0.775 (95% CI, 0.685-0.842, $P < 0.001$) in all MB vessels, 0.781 (95% CI, 0.684-0.850, $P < 0.001$) in superficial MB, 0.800 (95% CI, 0.503-0.928, $P < 0.001$) in deep MB, 0.756 (95% CI, 0.617-0.849, $P < 0.001$) in short MB, 0.789 (95% CI, 0.652-0.876, $P < 0.001$) in long MB, 0.631 (95% CI, 0.417-0.779, $P < 0.001$) in the 50% to 69% stenosis group and 0.777 (95% CI, 0.638-0.867, $P < 0.001$) in the ≥ 70% stenosis group. Bland-Altman plots demonstrated a slight mean difference between FFR and CT-FFR of 0.014 in all MB vessels and the ≥ 70% stenosis group, 0.013 in the 50% to 69% stenosis group, 0.019 in the superficial, deep and short MB groups, and 0.007 in the long MB group.

Discussion

This retrospective Chinese multicentre study investigated the diagnostic performance of CT-FFR based on ML algorithm to detect functional ischemia in patients with LAD MB and concomitant proximal atherosclerotic disease, using invasive FFR as the reference standard. Our study demonstrated that this ML-based CT-FFR has high diagnostic performance in the diagnosis of functional ischemia in vessels

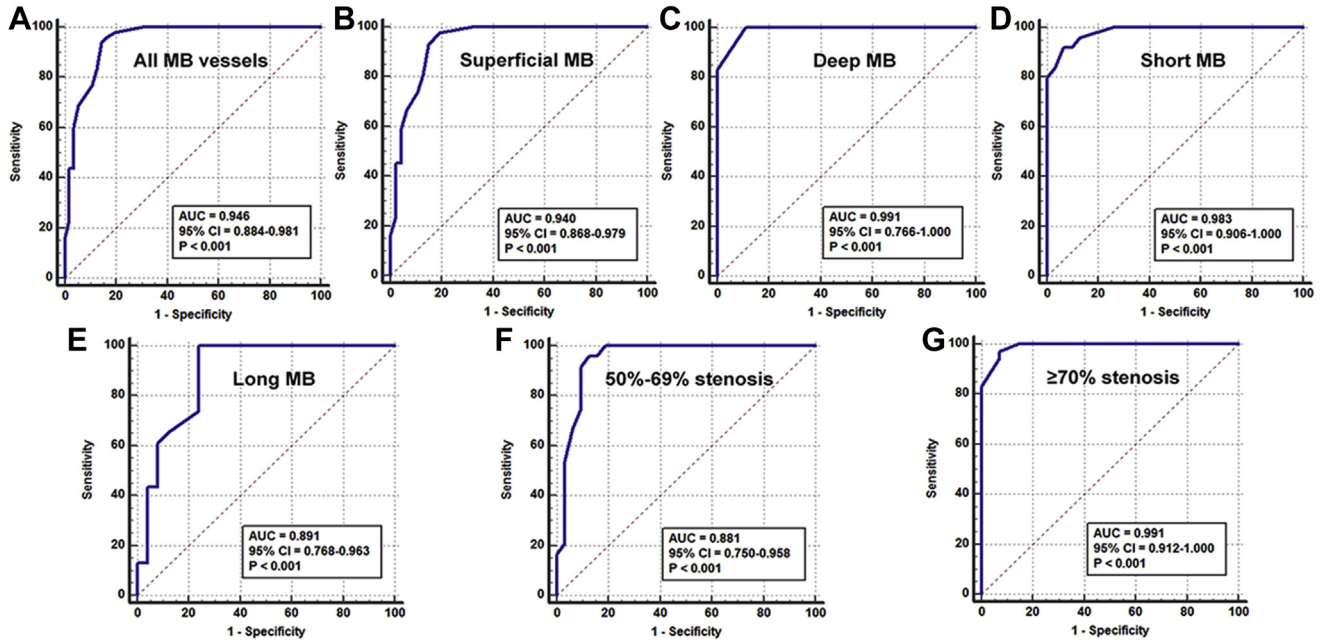

Figure 3. Per-vessel receiver operating characteristic (ROC) analysis of coronary computed tomography angiography derived fractional flow reserve (CT-FFR) in predicting hemodynamically significant stenosis (invasive FFR $\leq$ 0.80) for all MB vessels (**A**), superficial MB (**B**), deep MB (**C**), short MB (**D**), long MB (**E**), the 50% to 69% stenosis group (**F**), and the $\geq$ 70% stenosis group (**G**). AUC, area under the receiver operating characteristic curve; CI, confidence interval; MB, myocardial bridging.

with MB and concomitant proximal atherosclerotic disease, regardless of the length and depth of MB, with a relatively low PPV for patients with proximal atherosclerotic lesions of $<$ 70% stenosis.

In several previous studies, the general diagnostic performance of CT-FFR based on ML method has been described with sensitivities and specificities ranging from 0.79 to 0.91 and 0.76 to 0.96, respectively, regardless of the presence of MB.[12-14,31,32] Our Chinese multicentre study also verified the diagnostic performance of this ML-based CT-FFR for noninvasive evaluation of functionally significant coronary disease with similar sensitivity, specificity, and AUC of 0.96, 0.84 and 0.95, respectively, suggesting that this advanced technique is promising for determining functional ischemia in a broad population, including patients with MB. Although the PPVs of CT-FFR in the $<$ 50% stenosis group and the 50% to 69% stenosis group were only 0.50 and 0.59, respectively, in the current study, the accuracies, sensitivities, specificities, and NPVs for the $<$ 50% stenosis group and the 50% to 69% stenosis group were high. Moreover, there was only a slight inconsistency between CT-FFR values and invasive FFR, with a mean difference of 0.013 in the 50% to 69% stenosis group. Previous studies have also shown that CT-FFR has high diagnostic performance to identify ischemia for lesions with intermediate stenosis (30% to 69%) with a relatively low PPV (0.41 and 0.63).[33,34] In our mismatch cases, 81.8% (9 of 11) of CT-FFR values ranged from 0.75 to 0.85. Only 2 cases with CT-FFR beyond the range of 0.75 to 0.85 were found to have relatively long MBs, which may be a factor affecting diagnostic accuracy. In addition, bifurcation lesions with positive remodelling were reported to contribute to the mismatch between CT-FFR and invasive FFR; thus, particular attention should be paid when using CT-FFR in this condition.[35] Our mismatch group comprised 72.7% (8 of 11) of such lesions.

MB is traditionally known as a benign incidental finding on autopsy or angiography. Nevertheless, a small number of patients without obstructive CAD develop various clinical complications including stable and variant angina, acute coronary syndrome, and even sudden death. These coronary syndromes were attributed to the disordered coronary hemodynamics and microvascular dysfunction caused by tunnelled artery compression, which may further influence the coronary flow reserve. However, the dynamic stenosis caused by extravascular compression and intramyocardial tension, complex hemodynamics, and noncircular lumen morphology of MB may limit the utility of intracoronary physiology techniques. FFR is the average of systolic and diastolic pressure gradients. The tunnelled coronary artery compression during systole may result in a higher mean coronary pressure distal to the MB than the aortic pressure.[32] Previous studies showed that diastolic FFR (dFFR) and instantaneous wave-free ratio (iFR) might be better tools to detect hemodynamically significant stenosis in patients with MB.[19,36] Although the clinical value of CT-FFR seems to be independent of the presence of MB, as previous studies did not regard MB as an exclusion criterion, the diagnostic performance of CT-FFR in this setting is unclear. We, for the first time, investigated the role of CT-FFR in the evaluation of patients with MB in a relatively large sample size, showing high diagnostic performance and discrimination of ischemia by CT-FFR in the presence of

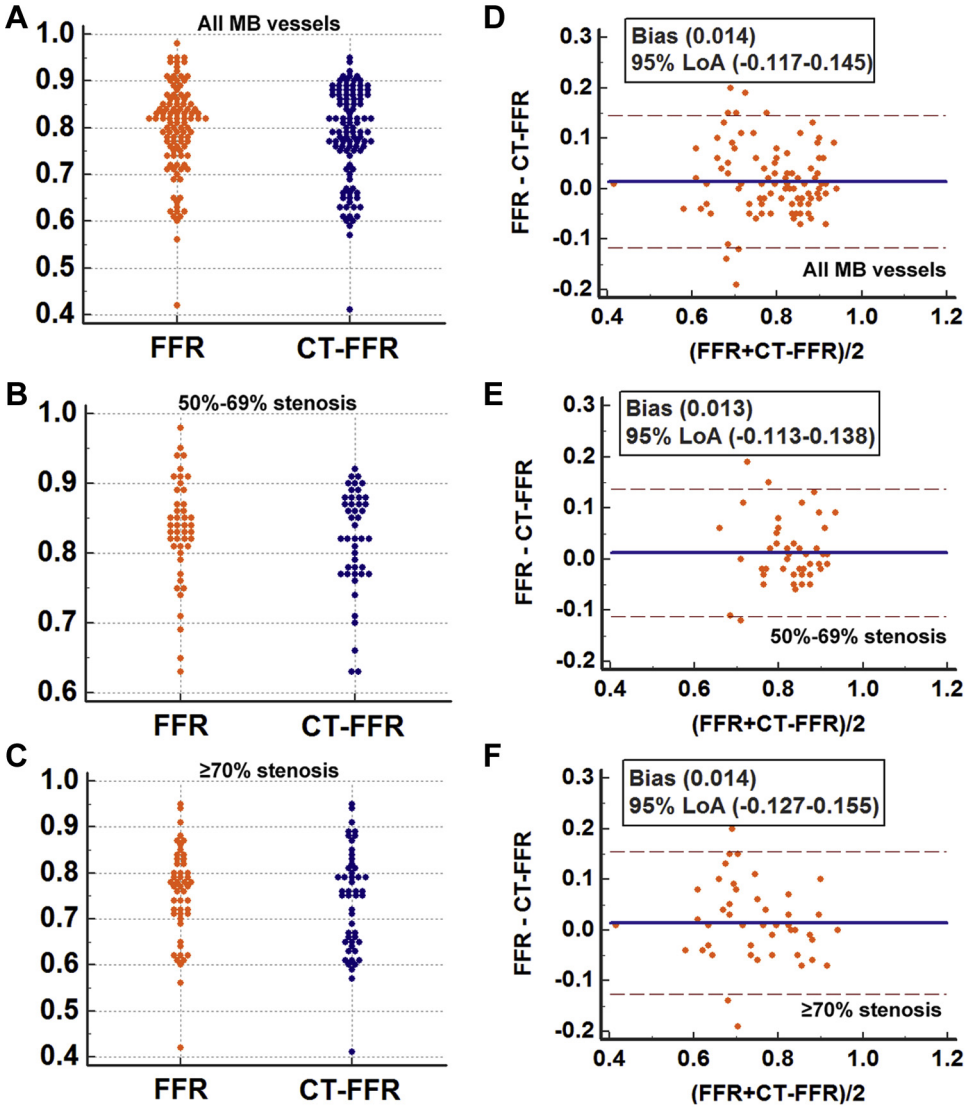

Figure 4. Comparisons between coronary computed tomography angiography derived fractional flow reserve (CT-FFR) and invasive FFR for all myocardial bridging (MB) vessels and different degrees of coronary stenosis groups. (**A-C**) Comparisons between CT-FFR and invasive FFR for all MB vessels (**A**), the 50% to 69% stenosis group (**B**), and the ≥ 70% stenosis group (**C**). (**D-F**) Bland-Altman plots and mean difference between CT-FFR and invasive FFR for all MB vessels (**D**), the 50% to 60% stenosis group (**E**), and the ≥ 70% stenosis group (**F**). LoA, limits of agreement.

MB. Although the diagnostic performance showed no significant difference between superficial and deep MB groups or between short and long MB groups, the diagnostic performance in vessels with deep MB needs further studies owing to the very small sample size. Further studies are needed to assess the specific relationship between the diagnostic performance of CT-FFR and MB features, in addition to MB depth and length.

Limitations

There are several limitations to the multicentre study that should be mentioned. First, this is a retrospective study with relatively small sample size, especially the number of deep MB. Second, 1 of the core principles for computing FFR is the predictability of the hyperemic response to adenosine; the nitroglycerin protocol used in our study for the acquisition of cCTA may have led to incomplete vasodilation in some patients. Third, in this study, we did not analyze the interobserver agreement or include patients without MB as controls. Fourth, only 1 patient with LAD MB without proximal plaque received invasive FFR in this retrospective cohort because most patients with MB are usually recommended for medical management rather than ICA in clinical setting. However, CT-FFR showed good diagnostic performance in 9 patients without obstructive LAD CAD (8 patients with non-obstructive LAD CAD, and 1 had no proximal LAD atherosclerotic plaque) and a "clean" study population should

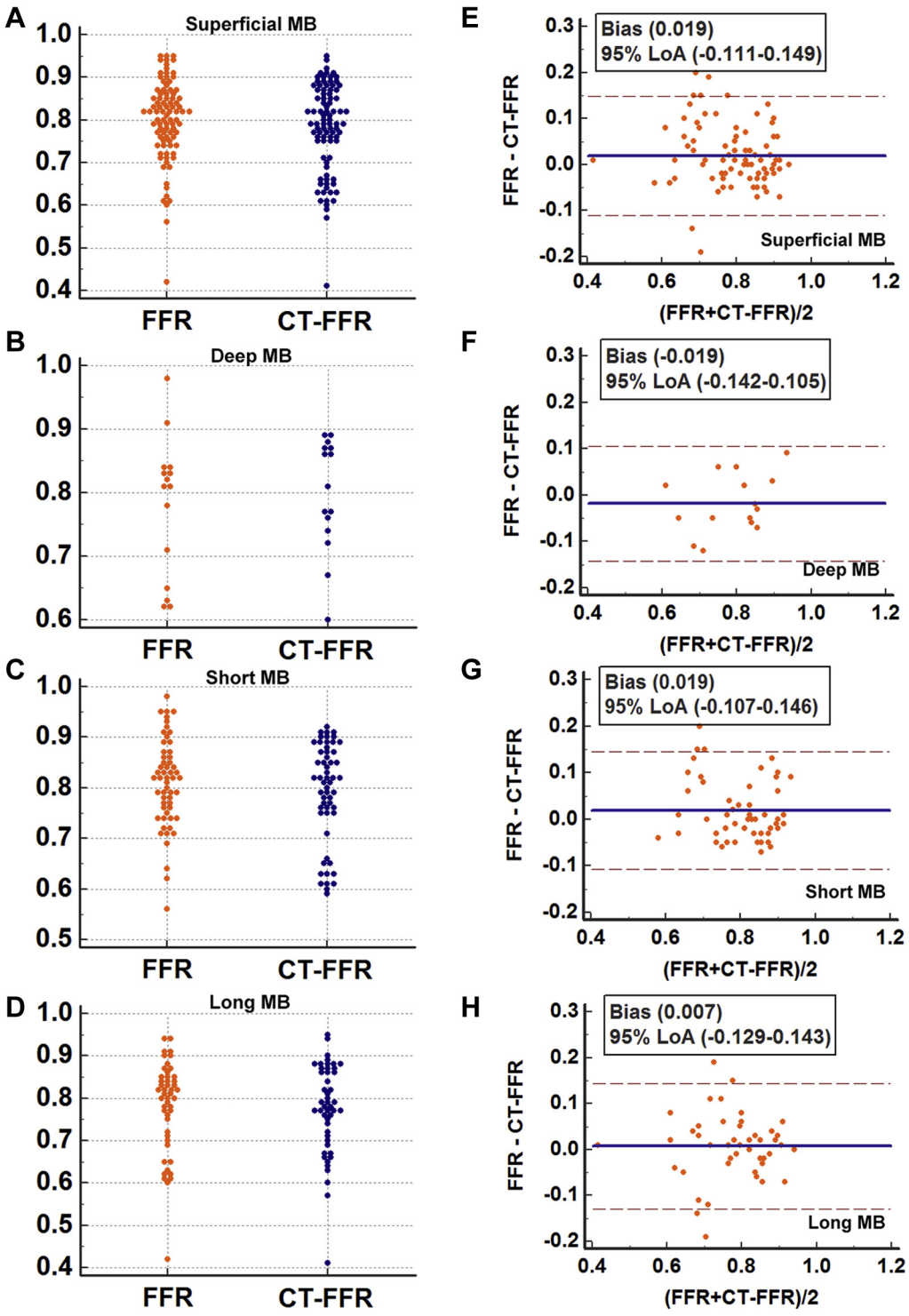

Figure 5. Comparisons between coronary computed tomography angiography derived fractional flow reserve (CT-FFR) and invasive FFR for different myocardial bridging (MB) groups. (**A-D**) Comparisons between CT-FFR and invasive FFR for superficial MB (**A**), deep MB (**B**), short MB (**C**), and long MB (**D**). (**E-H**) Bland-Altman plots and mean difference between CT-FFR and invasive FFR for superficial MB (**E**), deep MB (**F**), short MB (**G**), and long MB (**H**). LoA, limits of agreement.

be set to reduce the impact of CAD in a future study. Fifth, in the current study, invasive FFR was calculated in the rest condition; however, the best tool to evaluate the functional impact of MB is diastolic invasive FFR quantification with dobutamine stress owing to documentation of the flow-limiting effect of MB, particularly in the high heart rate condition. Finally, the overall diagnostic performance of CT-FFR also varies according to the image quality of cCTA.

Conclusions

Our study shows that ML-based CT-FFR has high diagnostic performance to identify functional ischemia in vessels with MB and concomitant proximal atherosclerotic disease compared with invasive FFR. However, the findings from this observational study do not support the clinical use of CT-FFR in this particular setting but rather the need for a properly designed and powered study to get stronger and more robust results in this specific setting.

Funding Sources

This study was supported by The National Key Research and Development Program of China (2017YFC0113400 for L.J.Z.).

Disclosures

Dr Schoepf is a consultant for and/or receives research support from Astellas, Bayer, General Electric, Guerbet, HeartFlow, and Siemens Healthineers. The other authors have no conflicts of interest to disclose.

References

1. De Bruyne B, Fearon WF, Pijls NH, et al. Fractional flow reserve-guided PCI for stable coronary artery disease. N Engl J Med 2014;371:1208-17.
2. Wijns W, Kolh P, Danchin N, et al. Guidelines on myocardial revascularization. Eur Heart J 2010;31:2501-55.
3. Pothineni NV, Shah NN, Rochlani Y, et al. U.S. trends in inpatient utilization of fractional flow reserve and percutaneous coronary intervention. J Am Coll Cardiol 2016;67:732-3.
4. Eftekhari A, Min J, Achenbach S, et al. Fractional flow reserve derived from coronary computed tomography angiography: diagnostic performance in hypertensive and diabetic patients. Eur Heart J Cardiovasc Imaging 2017;18:1351-60.
5. Min JK, Leipsic J, Pencina MJ, et al. Diagnostic accuracy of fractional flow reserve from anatomic CT angiography. JAMA 2012;308:1237-45.
6. Norgaard BL, Leipsic J, Gaur S, et al. Diagnostic performance of noninvasive fractional flow reserve derived from coronary computed tomography angiography in suspected coronary artery disease: the NXT trial (Analysis of Coronary Blood Flow Using CT Angiography: Next Steps). J Am Coll Cardiol 2014;63:1145-55.
7. Kawaji T, Shiomi H, Morishita H, et al. Feasibility and diagnostic performance of fractional flow reserve measurement derived from coronary computed tomography angiography in real clinical practice. Int J Cardiovasc Imaging 2017;33:271-81.
8. Douglas PS, De Bruyne B, Pontone G, et al. 1-year outcomes of FFRCT-guided care in patients with suspected coronary disease: the PLATFORM Study. J Am Coll Cardiol 2016;68:435-45.
9. Tesche C, De Cecco CN, Albrecht MH, et al. Coronary CT angiography-derived fractional flow reserve. Radiology 2017;285:17-33.
10. Duguay TM, Tesche C, Vliegenthart R, et al. Coronary computed tomographic angiography-derived fractional flow reserve based on machine learning for risk stratification of non-culprit coronary narrowings in patients with acute coronary syndrome. Am J Cardiol 2017;120:1260-6.
11. Kruk M, Wardziak Ł, Demkow M, et al. Workstation-based calculation of CTA-based FFR for intermediate stenosis. JACC Cardiovasc Imaging 2016;9:690-9.
12. Itu L, Rapaka S, Passerini T, et al. A machine-learning approach for computation fractional flow reserve from coronary computed tomography. J Appl Physiol (1985) 2016;121:42-52.
13. Tesche C, De Cecco CN, Baumann S, et al. Coronary CT angiography-derived fractional flow reserve: machine learning algorithm versus computational fluid dynamics modeling. Radiology 2018;288:64-72.
14. Röther J, Moshage M, Dey D, et al. Comparison of invasively measured FFR with FFR derived from coronary CT angiography for detection of lesion-specific ischemia: results from a PC-based prototype algorithm. J Cardiovasc Comput Tomogr 2018;12:101-7.
15. Tarantini G, Migliore F, Cademartiri F, Fraccaro C, Iliceto S. Left anterior descending artery myocardial bridging: a clinical approach. J Am Coll Cardiol 2016;68:2887-99.
16. Corban MT, Hung OY, Eshtehardi P, et al. Myocardial bridging: contemporary understanding of pathophysiology with implications for diagnostic and therapeutic strategies. J Am Coll Cardiol 2014;63:2346-55.
17. Javadzadegan A, Moshfegh A, Fulker D, et al. Development of a computational fluid dynamics model for myocardial bridging. J Biomech Eng 2018:140.
18. Yamada R, Tremmel JA, Tanaka S, et al. Functional versus anatomic assessment of myocardial bridging by intravascular ultrasound: impact of arterial compression on proximal atherosclerotic plaque. J Am Heart Assoc 2016;5:e001735.
19. Escaned J, Cortés J, Flores A, et al. Importance of diastolic fractional flow reserve and dobutamine challenge in physiologic assessment of myocardial bridging. J Am Coll Cardiol 2003;42:226-33.
20. Maeda K, Schnittger I, Murphy DJ, et al. Surgical unroofing of hemodynamically significant myocardial bridges in a pediatric population. J Thorac Cardiovasc Surg 2018;156:1618-26.
21. Chatzizisis YS, Giannoglou GD. Myocardial bridges spared from atherosclerosis: overview of the underlying mechanisms. Can J Cardiol 2009;25:219-22.
22. Zhou F, Tang CX, Schoepf UJ, et al. Fractional flow reserve derived from CCTA may have a prognostic role in myocardial bridging. Eur Radiol 2019;29:3017-26.
23. Ishikawa Y, Akasaka Y, Suzuki K, et al. Anatomic properties of myocardial bridge predisposing to myocardial infarction. Circulation 2009;120:376-83.
24. Konen E, Goitein O, Sternik L, Eshet Y, Shemesh J, Di Segni E. The prevalence and anatomical patterns of intramuscular coronary arteries: a coronary computed tomography angiographic study. J Am Coll Cardiol 2007;49:587-93.
25. Cerci R, Vavere AL, Miller JM, et al. Patterns of coronary arterial lesion calcification by a novel, cross-sectional CT angiographic assessment. Int J Cardiovasc Imaging 2013;29:1619-27.
26. Sekimoto T, Akutsu Y, Hamazaki Y, et al. Regional calcified plaque score evaluated by multidetector computed tomography for predicting the addition of rotational atherectomy during percutaneous coronary intervention. J Cardiovasc Comput Tomogr 2016;10:221-8.
27. Achenbach S, Rudolph T, Rieber J, et al. Performing and interpreting fractional flow reserve measurements in clinical practice: an expert consensus document. Interv Cardiol 2017;12:97-109.

28. Collet C, Miyazaki Y, Ryan N, et al. Fractional flow reserve derived from computed tomographic angiography in patients with multivessel CAD. J Am Coll Cardiol 2018;71:2756-69.

29. Aleksandra C, Olga T, Agnieszka B-R, et al. Severity scores for Ebstein anomaly: credibility and usefulness of echocardiographic versus magnetic resonance assessments of the Celermajer Index [e-pub ahead of print]. Can J Cardiol, https://doi.org/10.1016/j.cjca.2019.08.003.

30. DeLong ER, DeLong DM, Clarke-Pearson DL. Comparing the areas under two or more correlated receiver operating characteristic curves: a nonparametric approach. Biometrics 1988;44:837-45.

31. Coenen A, Kim YH, Kruk M, et al. Diagnostic accuracy of a machine-learning approach to coronary computed tomographic angiography-based fractional flow reserve: result from the MACHINE consortium. Circ Cardiovasc Imaging 2018;11:e007217.

32. Tang CX, Wang YN, Zhou F, et al. Diagnostic performance of fractional flow reserve derived from coronary CT angiography for detection of lesion-specific ischemia: a multi-center study and meta-analysis. Eur J Radiol 2019;116:90-7.

33. Nakazato R, Park HB, Berman DS, et al. Noninvasive fractional flow reserve derived from computed tomography angiography for coronary lesions of intermediate stenosis severity: results from the DeFACTO study. Circ Cardiovasc Imaging 2013;6:881-9.

34. Donnelly PM, Kolossváry M, Karády J, et al. Experience with an on-site coronary computed tomography-derived fractional flow reserve algorithm for the assessment of intermediate coronary stenoses. Am J Cardiol 2018;121:9-13.

35. Osawa K, Miyoshi T, Miki T, et al. Coronary lesion characteristics with mismatch between fractional flow reserve derived from CT and invasive catheterization in clinical practice. Heart Vessels 2017;32:390-8.

36. Tarantini G, Barioli A, Nai Fovino L, et al. Unmasking myocardial bridge-related ischemia by intracoronary functional evaluation. Circ Cardiovasc Interv 2018;11:e006247.

Supplementary Material

To access the supplementary material accompanying this article, visit the online version of the *Canadian Journal of Cardiology* at www.onlinecjc.ca and at https://doi.org/10.1016/j.cjca.2019.08.026.